Available online at www.sciencedirect.com

ScienceDirect

Journal of Terramechanics 71 (2017) 45–56

Journal of Terramechanics

www.elsevier.com/locate/jterra

Bayesian calibration of Vehicle-Terrain Interface algorithms for wheeled vehicles on loose sands

Ian Dettwiller [a], Masoud Rais-Rohani [a,e], Farshid Vahedifard [b,*], George L. Mason [c], Jody D. Priddy [d]

[a] Dept. of Aerospace Engineering and Center for Advanced Vehicular Systems, Mississippi State University, Mississippi State, MS 39762, USA
[b] Dept. of Civil and Environmental Engineering and Center for Advanced Vehicular Systems, Mississippi State University, Mississippi State, MS 39762, USA
[c] Center for Advanced Vehicular Systems, Mississippi State University, Mississippi State, MS 39762, USA
[d] U.S. Army Engineer Research and Development Center, 3909 Halls Ferry Road, Vicksburg, MS 39180, USA
[e] Department of Mechanical Engineering, The University of Maine, Orono, ME 04469, USA

Received 12 May 2016; received in revised form 31 January 2017; accepted 14 February 2017
Available online 19 March 2017

Abstract

The Vehicle-Terrain Interface (VTI) model is commonly used to predict off-road mobility to support virtual prototyping. The Database Records for Off-road Vehicle Environments (DROVE), a recently developed database of tests conducted with wheeled vehicles operating on loose, dry sand, is used to calibrate three equations used within the VTI model: drawbar pull, traction, and motion resistance. A two-stage Bayesian calibration process using the Metropolis algorithm is implemented to improve the performance of the three equations through updating of their coefficients. Convergence of the Bayesian calibration process to a calibrated model is established through evaluation of two indicators of convergence. Improvements in root-mean square error (RMSE) are shown for all three equations: 17.7% for drawbar pull, 5.5% for traction, and 23.1% for motion resistance. Improvements are also seen in the coefficient of determination (R^2) performance of the equations for drawbar pull, 2.8%, and motion resistance, 2.5%. Improvements are also demonstrated in the coefficient of determination for drawbar pull, 2.8%, and motion resistance, 2.5%, equations, while the calibrated traction equation performs similar to the VTI equation. A randomly selected test dataset of about 10% of the relevant observations from DROVE is used to validate the performance of each calibrated equation.

Keywords: Off-road mobility; Vehicle Terrain Interface (*VTI*) model; Bayesian calibration; Metropolis algorithm; Sand; Drawbar pull (*DP*); Traction; Motion resistance; Database Records for Off-road Vehicle Environments (DROVE)

1. Introduction

Off-road vehicles serve a crucial role for both civilian and military transportations. Effective modeling of off-road vehicle mobility at diverse fidelities and on various terrains is an important task for many vehicle design applications. Two popular off-road vehicle performance models are the NATO Reference Mobility Model (NRMM) (Ahlvin and Haley, 1992; Vong et al., 1999) and the Virtual Autonomous Navigation Environment (VANE) (Jones et al., 2007), although other models have also been used (Lee, 2015; Taheri et al., 2015). These models relate vehicle performance, environmental conditions, and the terrain.

The Vehicle Terrain Interface (VTI) model is a high-resolution empirical model that addresses the interactions at the traction-terrain element interface and was developed as part of the NRMM and VANE models. The VTI serves

* Corresponding author.
E-mail addresses: idd4@msstate.edu (I. Dettwiller), masoud.raisrohani@maine.edu (M. Rais-Rohani), farshid@cee.msstate.edu (F. Vahedifard), mason@cavs.msstate.com (G.L. Mason), Jody.D.Priddy@erdc.dren.mil (J.D. Priddy).

http://dx.doi.org/10.1016/j.jterra.2017.02.003
0022-4898/

Nomenclature

VTI	Vehicle Terrain Interface
DROVE	Database Records for Off-road Vehicle Environments
DP	drawbar pull
NRMM	NATO Reference Mobility Model
VANE	Virtual Autonomous Navigation Environment
F_t	net tractive effort
R	total motion resistance
ISTVS	International Society for Terrain-Vehicle Systems
DBP	coefficient of drawbar pull
T	coefficient of traction
MR	coefficient of motion resistance
s	slip
r_R	rolling radius
ω	angular velocity of the wheel
V_v	forward velocity of the vehicle
W	vehicle or wheel load
α	steering angle
N_s	sand numeric
G	penetration gradient
b	tire width
h	section height
δ	difference between loaded and unloaded section heights
x_i	general coefficients for calibration
$N_{s,u}$	unpowered sand numeric
CI_{0-15}	average soil cone index from 0 to 15 cm
BC	Bayesian calibration
θ	calibration parameters
ϕ	variable parameters
η	model output
ϵ	observation error
$L(D\|\theta)$	likelihood function
$P(\theta)$	prior distribution
$P(\theta\|D)$	posterior distribution
D	data for calibration
PDF	probability density function
v	variance of an observation
y	property being modeled
θ_{can}	candidate vector of calibration parameters
θ_0	previous vector of calibration parameters
V	variance-covariance matrix
P_{can}	prior distribution of candidate vector
L_{can}	likelihood function of candidate vector
P_0	prior distribution of previous vector
L_0	likelihood function of previous vector
γ	Metropolis ratio
n	Length of the Markov chain
θ^n	final set of accepted calibration parameters from Markov Chain
Min_{ref}	minimum for reflection
Max_{ref}	maximum for reflection
σ	standard deviation
a	term to adjust step size in the Metropolis algorithm
μ	mean
c	second term to adjust step size of the Metropolis algorithm
UB	upper bound
LB	lower bound
RMSE	root-mean square error
R^2	coefficient of determination
CAVS	Center for Advanced Vehicular Systems

as a practical tool to support virtual prototyping of off-road vehicles without the computational cost of the larger models, a valuable part of the computer-aided design process (MacLeod, 2001). One advantage of the VTI model is its flexibility, being able account for both tracked and wheeled vehicles, steering conditions, and whether or not the vehicle is operating on ridged or fixed materials (Rohde et al., 2009). Steering is supported in the VTI model by equations for turning of the wheel on a deformable media developed by Melzer (1976), reorganized by Durham (1976) and implemented in the VTI (Jones et al., 2007).

The empirical nature of the VTI model allows for, or even necessitates, updating of the VTI equations as new data become available through either laboratory or field-testing. A recent effort to evaluate the performance of vehicle mobility models resulted in the Database Records for Off-road Vehicle Environments (DROVE) (Vahedifard et al., 2016, 2017), and suggested the performance of the VTI model could be improved for loose, dry sands.

In the current study, a two-stage Bayesian calibration technique was employed to improve the performance of the drawbar pull, traction, and motion resistance equations within the VTI model. The following sections of this paper include a brief discussion of the VTI model and the equations considered, an overview of Bayesian calibration, and results including the calibrated algorithms and their performance.

2. Vehicle performance parameters

Three vehicle performance parameters described in the VTI model are considered in this effort: drawbar pull force (DP), gross traction force (F_p), and total motion resistance (R) defined according to the ISTVS standards (Meyer et al., 1977; Priddy, 1999). Each parameter is normalized by weight to give the coefficient of drawbar pull (DBP), coefficient of traction (T), and coefficient of motion resistance (MR) illustrated for non-steered tires in Fig. 1.

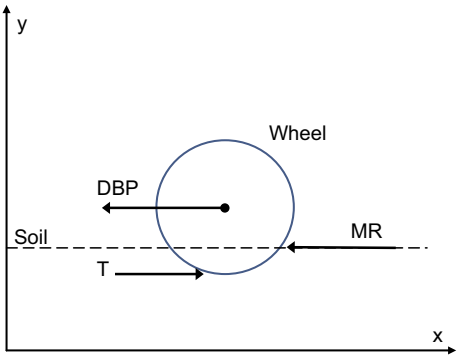

Fig. 1. Tire forces and vehicle parameters for non-steered vehicle.

2.1. Drawbar pull

A common approach to demonstrating vehicle, or tire, performance is the drawbar pull test, which measures the vehicle's pulling capacity (Freitag and Knight, 1964). Drawbar pull tests are usually conducted by attaching load cells parallel to the ground along the axis of the pulling tractive elements of the test platform. In the field, these tests are sometimes initiated with the test vehicle traveling slower than 2 m/s (Schreiner et al., 1985) at or near zero slip and being pulled to a stop, and sometimes conducted starting near zero slip and continuing until slip reaches about 50%. Slip, (s), begins near zero percent for field tests and is preprogrammed during laboratory tests. Slip, a state variable, expresses how wheel velocity, the rolling radius (r_R) times the angular velocity of the wheel (ω), differs from the forward velocity of the vehicle, V_v using the equation (Meyer et al., 1977) $s = (r_R\omega - V_v)/r_R\omega$. For field tests, s is found by comparing the distance traveled by the wheel and the distance traveled by the vehicle, where the distance traveled by the wheel is a function of r_R and ω. The longitudinal wheel velocity for single wheeled laboratory tests (Turnage, 1972) is usually kept between 1 and 5.5 m/s to define the relationship between longitudinal wheel velocity and vehicle performance parameters. Several studies have been conducted to demonstrate the relationship between wheel geometry (width, diameter, etc.), longitudinal wheel velocity, and parameters such as DBP and s (Durham, 1976; Turnage, 1972) with evidence presented suggesting the effects of longitudinal wheel velocity do not scale according to tire size (Turnage, 1972). One of the advantages of laboratory testing over field-testing is the ability to either vary the slip or hold slip relatively constant, while maintaining a relatively constant slip is more difficult in field tests.

The lumped parameter solution used in the VTI model for predicting DBP (Durham, 1976) of a wheel operating on sand is

$$\begin{aligned}\mathrm{DBP} &= \frac{DP}{W} \\ &= 0.69 - \frac{0.01}{s} - 1.42\alpha^{0.6+3.1s} \\ &\quad - \frac{\left(0.69 - \frac{0.01}{s} - 1.42\alpha^{0.6+3.1s}\right)(10.8 - 16\alpha^{0.8})}{N_s - \frac{2.23}{\frac{1}{s^3}} + \frac{15}{s}\alpha^3 + 10.8 - 16\alpha^{0.8}}\end{aligned} \tag{1}$$

where DBP is defined as the drawbar pull of the vehicle, DP, normalized by vertical vehicle or wheel load, W. The equation accounts for steering directly through the tire angle, α, and soil physical properties through the sand numeric N_s defined for loose sandy soils (Turnage, 1972) as

$$N_s = \frac{G(bd)^{\frac{3}{2}}\delta}{Wh} \tag{2}$$

where G represents the penetration gradient, itself a measure of soil strength. Tire geometry is captured through the unloaded tire dimensions width, b, diameter, d, and section height, h. The δ term is defined as the difference between the loaded and unloaded section heights. The empirical coefficients in Eq. (1) can be assessed using data from existing of future laboratory or field tests and are easily adjusted to improve the predictive performance of the equations. These coefficients are replaced with x_i, $i = 1, \ldots, 10$, in the coefficient form of Eq. (1), given as

$$\begin{aligned}\mathrm{DBP} &= x_1 - \frac{x_2}{s} - x_3\alpha^{x_4+x_5 s} \\ &\quad - \frac{\left(x_1 - \frac{x_2}{s} - x_3\alpha^{x_4+x_5 s}\right)(x_6 - x_7\alpha^{x_8})}{N_s - \frac{x_9}{\frac{1}{s^3}} + \frac{x_{10}}{s}\alpha^3 + x_6 - x_7\alpha^{x_8}}\end{aligned} \tag{3}$$

2.2. Traction

Gross traction is the torque delivered to the wheel divided by the effective radius of the wheel. If direct measurements of DP and R are taken for field tests, then F_p must be measured indirectly from the applied torque, active radius of the tire, and tire deformation (Priddy, 1999). The T equation used in the VTI model for wheeled vehicles in loose sands (Jones et al., 2007) is given as

Table 1
Properties for loose dry sands used in the study.

Soil type	Dry unit weight (kN/m^3)		Void ratio		Relative density (%)		Avg. cone penetration resistance (kN/m^2)		Avg. penetration resistance gradient (MN/m^3)	
	Min	Max	Min	Max	Min	Max	Min	Max	Min	Max
Yuma sand (SP-SM)	13.773	16.282	0.610	0.901	5.8	99.4	28	475	0.3	5.8
Mortar sand (SP)	13.881	16.422	0.595	0.887	6.3	93.2	35	455	0.4	6.3

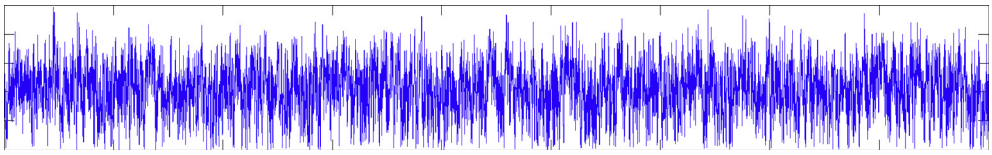

Fig. 2. Converged trace plot.

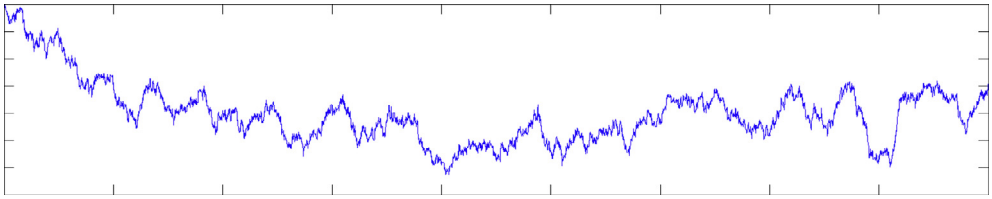

Fig. 3. Non-converged trace plot.

1. Define model, $\eta(\theta,\phi)$ (Eqs. (3), (5), and (8)), and data, D (DROVE).
2. Select chain length, n.
3. Select prior probability distribution for parameters, $P(\theta)$.
4. Define Variance-Covariance matrix of the proposal distribution, V.
5. Define likelihood function as a function of the difference between model and data
$$L(D|\theta) \sim (\eta(\theta,\phi) D)$$
6. Select a starting point in the coefficient space, θ_0.
7. Generate θ_{can} from Multivariate Gaussian Distribution, (θ_0, V).
8. Reflect infeasible vectors into the design space.
   a. $Min_{ref} = \min(0, \theta_{can} - \theta_{min})$
   b. $Max_{ref} = \max(0, \theta_{can} - \theta_{max})$
   c. $\theta_{can} = \theta_{can} - 2Min_{ref} - 2Max_{ref}$
9. Calculate Metropolis ratio, $\gamma = P_{can}L_{can}/(P_0L_0)$
10. Accept if $\gamma > 1$ or randomly with probability γ otherwise
11. If accepted, $\theta_0 = \theta_{can}$; otherwise, $\theta_0 = \theta_0$
12. Repeat 6 through 11 n times to obtain posterior sample, θ^n.
13. Determine updated coefficients, $x_i = \text{mean}(\theta_i^n)$

Fig. 4. Metropolis algorithm.

$$T = \frac{F_p}{W} = 0.66 - \frac{0.66\left(4.71 + \frac{1.72}{s}\right)}{N_s + 10 + \left(4.71 + \frac{1.72}{s}\right)} \tag{4}$$

where F_p is normalized by W to give T. Note that the traction equation does not account for steering, although both s and N_s appear as they did for DBP. The coefficient form of the T equation to be calibrated is given as

$$T = x_1 - \frac{x_2\left(x_3 + \frac{x_4}{s}\right)}{N_s + x_5 + \left(x_6 + \frac{x_7}{s}\right)} \tag{5}$$

2.3. Unpowered motion resistance

Motion resistance encompasses the internal and external forces which restrict a vehicle's forward motion. Measurement of R in the laboratory is conducted directly during unpowered tests with a load cell mounted in the same manner as with the DP tests. During powered tests, R is an indirect measurement of the difference between measured F_p and DP. The resistance of loose soil on unpowered wheel motion depends on the rate at which the soil deforms (Schreiber and Kutzbach, 2008). The VTI equation for MR (Turnage, 1995) is given as

$$\begin{aligned} MR &= \frac{R}{W} \\ &= 0.44 - 0.002287N_{s,u} \\ &\quad + \sqrt{(0.44 - 0.002287N_{s,u})^2 + 0.0000457N_{s,u} + 0.008} \end{aligned} \tag{6}$$

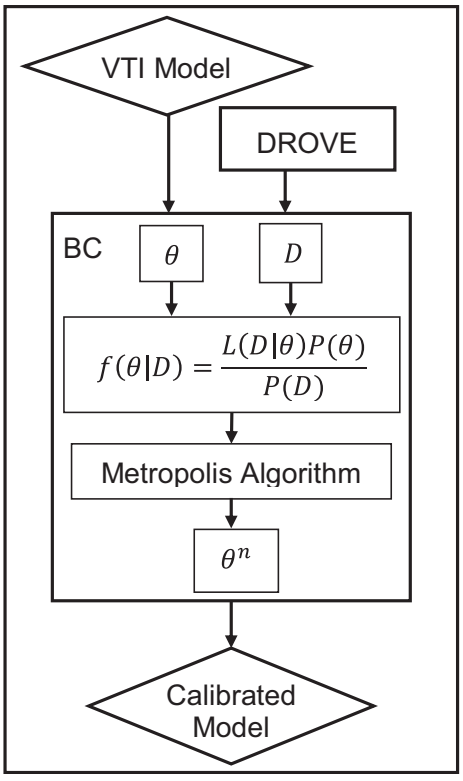

Fig. 5. Bayesian calibration process to develop the calibrated model.

where R is normalized by W to give MR, as was done for DBP and T.

The unpowered sand numeric, $N_{s,u}$, is defined as

$$N_{s,u} = \frac{\left(\frac{CI_{0-15}(bd)^{\frac{3}{2}}}{\left(1-\frac{a}{h}\right)^3 W}\right)}{1-\frac{b}{d}} \quad (7)$$

and considers a plethora of information about the soil-tire interface, including the average soil cone index (CI) for a depth range of 0–15 cm, CI_{0-15}. The coefficient form of the unpowered MR model to be calibrated in the current study is given as

$$MR = x_1 - x_2 N_{s,u} + \sqrt{(x_3 - x_4 N_{s,u})^2 + x_5 N_{s,u} + x_6} \quad (8)$$

Table 2
Gaussian prior distributions for exploration of drawbar pull equation.

DBP	x_1	x_2	x_3	x_4	x_5	x_6	x_7	x_8	x_9	x_{10}
μ	0.5	0.01	1.5	0.5	3	10	15	0.8	2	15
σ_i^2	0.5	0.01	1	0.5	1	1	1	0.8	1	1

3. Database Records for Off-road Vehicle Environments (DROVE)

For calibration purposes, we use DROVE, a recently developed database of tests conducted with wheels operating on loose, dry sand (Vahedifard et al., 2016), to improve the performance of the drawbar pull, traction, and motion resistance models within the VTI model. Vahedifard et al. (2016) created DROVE using 5522 records describing a variety of laboratory and field tests of wheels in loose, dry sands similar to those shown in Table 1 (Melzer, 1971) where descriptions SP and SM define poorly-graded sands and coarse material with non-plastic or low-plasticity fines, respectively, according to The Unified Soil Classification System (1960).

Each record contains observations of test data (e.g. measured DP, F_p, R, etc.) and characterizing data for the soil and vehicles used. The database included tires of different overall diameters (35.7–124.5 cm), section widths (3.5–41 cm), section heights (3.56–30.5 cm), and inflation pressures, operating under various loading conditions (Null to 36.12 kN). The average loading for the tests was 7.53 kN with a standard deviation of 6.6 kN, although the distribution of tests was not symmetric (Vahedifard et al., 2016). Tests were conducted using a variety of sands defined as more than 50% of the material passing through a 4.75 mm sieve. The average CI_{0-15} of the soils was 263 kPa with a standard deviation of 250 kPa, resulting in a wide, although uneven, distribution of soil strengths (Vahedifard et al., 2016). Although 5522 records were available, not all technical reports considered the same parameters. Subsets of data for the three models were independently assembled to ensure a maximum amount of data for each one of the models by removing those records that did not contain all required inputs.

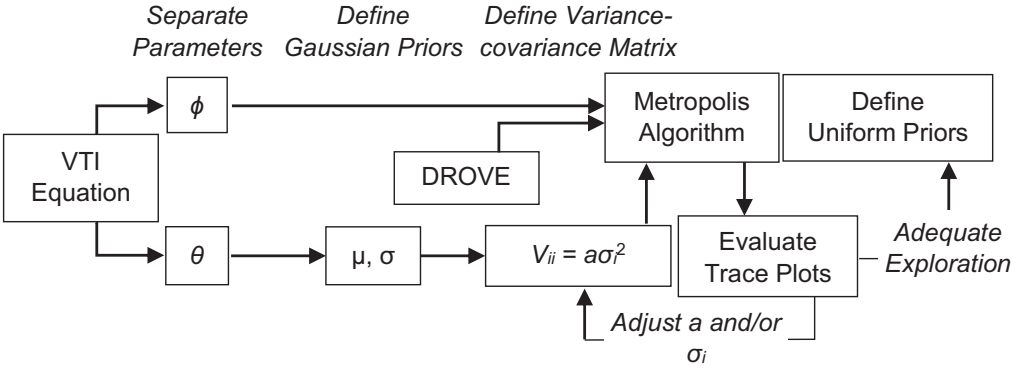

Fig. 6. First-stage calibration process.

Table 3
Initial and final exploration chain means for drawbar pull.

Model	x_1	x_2	x_3	x_4	x_5	x_6	x_7	x_8	x_9	x_{10}
Initial	0.5	0.01	1.5	0.5	3	10	15	0.8	2	15
Chain 1	0.542	−0.011	8.214	0.974	10.36	13.58	−6.39	3.40	1.23	16.24
Chain 2	0.568	−0.004	6.519	1.040	8.04	12.81	6.70	0.844	1.30	14.30
Chain 3	0.625	0.005	2.373	0.711	4.35	13.57	8.54	0.562	1.20	21.12
Chain 4	0.589	−0.002	12.71	1.510	9.68	13.70	28.86	1.74	1.21	−6.28
Chain 5	0.554	−0.008	3.597	0.831	6.95	13.46	19.94	1.41	1.23	4.17

Table 4
Original VTI values and prior distribution bounds for coefficients in drawbar pull equation.

DBP	x_1	x_2	x_3	x_4	x_5	x_6	x_7	x_8	x_9	x_{10}
VTI	0.69	0.01	1.42	0.6	3.1	10.8	16	0.8	2.23	15
LB	0.5	−0.02	1	0.5	3	10	−7	0.5	1	−7
UB	0.7	0.015	15	1.6	11	14	30	3.5	2.5	22

Table 5
Original VTI and mean values for coefficients in drawbar pull equation with uniform priors.

Model	x_1	x_2	x_3	x_4	x_5	x_6	x_7	x_8	x_9	x_{10}
Chain 1	0.53	−0.011	5.26	0.91	8.30	12.54	10.1	2	1.34	4.95
Chain 2	0.53	−0.011	5.36	0.91	8.35	12.53	10.3	2	1.33	5.35
Chain 3	0.53	−0.011	5.62	0.94	8.41	12.59	9.7	2	1.33	5.53
Average	0.53	−0.011	5.41	0.92	8.35	12.55	10.0	2	1.33	5.28

Table 6
Performance of calibrated drawbar pull equation.

Performance	Calibration set R^2	Calibration set RMSE	Test set R^2	Test set RMSE
VTI model	0.79	0.0739	0.827	0.0651
Calibrated model	0.81	0.0611	0.843	0.0540
% Improvement	2.82	17.3	2.0	17.0

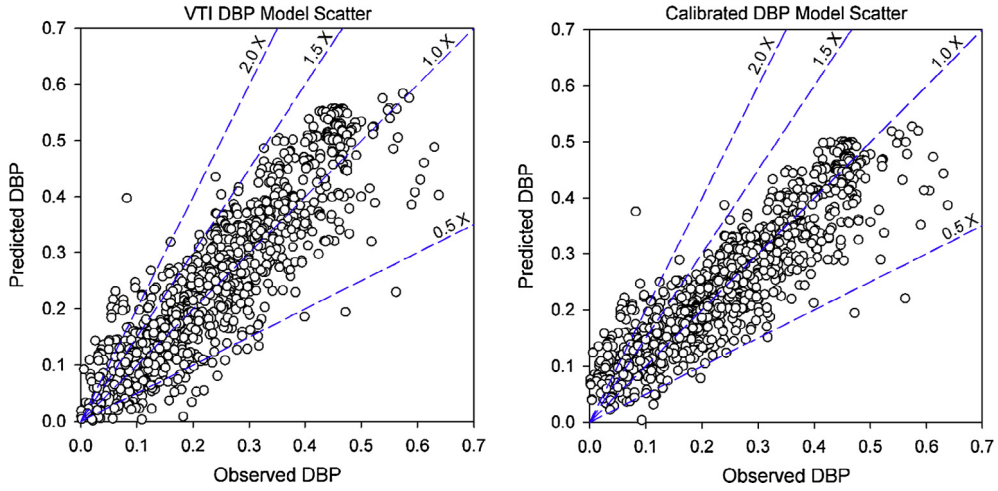

Fig. 7. VTI and calibrated model scatter plots for drawbar pull.

The DBP model required several dimensional and soil inputs, measured *DP*, slip, and steer angle data. The DBP dataset consisted of 1051 records from DROVE, of which 120, about 11% of the data, were randomly excluded from the calibration effort and set aside to validate the calibrated model (Stone, 1974). A major limitation of the data collected was the relatively few entries which included steer angle data, just 37 of the 1051 applicable records from

Table 7
Gaussian prior distributions for exploration of traction equation.

T	x_1	x_2	x_3	x_4	x_5	x_6	x_7
μ	1	1	5	3	8	5	3
σ_i^2	1	1	2.5	1.5	4	2.5	1.5

Table 8
Initial and final exploration chain means for traction.

Gaussian	x_1	x_2	x_3	x_4	x_5	x_6	x_7
Initial	1	1	5	3	8	5	3
Chain 1	0.73	0.39	1.08	5.77	10.41	−0.38	3.29
Chain 2	0.76	1.80	1.60	1.30	13.50	1.69	3.22
Chain 3	0.74	0.72	3.54	2.86	1.38	12.66	2.74
Chain 4	0.81	1.90	2.94	1.57	14.72	7.38	3.77
Chain 5	0.73	0.76	2.71	2.72	−2.93	15.87	2.83

DROVE, resulting in a significant obstacle to validating the DBP model. Sub-datasets were similarly created for T and MR. In total 1203 records were available for T, with 120 set aside for model validation (10%), and 1010 records for MR, with 101 (10%) observations set aside for model validation.

4. Bayesian calibration

Bayesian calibration (BC) utilizes Bayesian statistics to calibrate a model for a given dataset (Kennedy and O'Hagan, 2001; Van Oijen, 2008). The BC implementation in this study adjusts the coefficients of an equation to improve performance without changing the model structure. The calibrated equations presented should therefore be considered adjusted, rather than new, equations (Kennedy and O'Hagan, 2001). This also ensures the calibrated equations represent little to no increase in the computational cost of evaluation.

The first step in BC is the separation of all model parameters into two categories: calibration parameters and variable parameters. The vector of calibration parameters, θ, is those parameters to be adjusted and is considered unknown for calibration. The x_i terms in Eqs. (3), (5), and (8) make up θ for each equation. All other parameters are defined as variable parameters, ϕ, and are adjusted in the calibrated model to consider changes in the modeled system. Together θ and ϕ give the model output, $\eta(\theta, \phi)$, which is related to the true, physical property being modeled, y_i, through the equation $y_i = \eta_i(\theta, \phi_i) + \epsilon_i$ where ϵ_i is the error of observation i and ϕ_i is the vector of input parameters for observation i (O'Hagan, 2006).

Table 9
Original VTI values and prior distribution bounds for coefficients in traction equation.

T	x_1	x_2	x_3	x_4	x_5	x_6	x_7
VTI	0.66	0.66	4.71	1.72	10	4.71	1.72
LB	0.7	0.7	2.5	1.5	4	4	1.5
UB	0.81	1.5	5	3	18	12	4

Table 10
Original VTI and mean values for coefficients in traction equation with uniform priors.

Uniform	x_1	x_2	x_3	x_4	x_5	x_6	x_7
Chain 1	0.77	1.09	3.80	2.17	10.6	7.89	3.14
Chain 2	0.77	1.10	3.75	2.17	10.0	8.30	3.15
Chain 3	0.77	1.08	3.85	2.17	10.8	7.58	3.12
Average	0.77	1.09	3.80	2.17	10.5	7.93	3.14

BC is used to update terms in θ through Bayes' rule from probability theory, expressed as

$$P(\theta|D) = \frac{L(D|\theta)P(\theta)}{P(D)} \tag{9}$$

where $L(D|\theta)$ is the likelihood function, $P(\theta)$ is the prior probability density function (PDF), $P(D)$ is a scaling factor, defined by integrating $L(D|\theta)P(\theta)$ over the range of θ, and $P(\theta|D)$ is the posterior PDF. Bayesian statistics focuses on the probability of a random variable given a set of data (Lee, 2012), making it ideal for adjusting model coefficients. Any term considered unknown in the calibration stage, namely all terms in θ, must be assigned a prior PDF in BC, a non-trivial matter (Kass and Wasserman, 1996). A Gaussian likelihood function of the following form is used throughout the calibration process:

$$L(D|\theta) = \prod_{i=1}^{N} \frac{1}{v_i\sqrt{2\pi}} e^{-(D_i-\eta_i(\theta,\phi_i))^2/(2v_i)} \tag{10}$$

where v_i is the variance associated with observation i and N the total number of observations.

The posterior PDF contains the information about the final, updated parameters. This information is isolated for a single parameter by integrating across the domains of all the other parameters, a process that quickly becomes computationally expensive, or infeasible, as dimensionality increases. For example, determining the calibrated value of x_1 in Eq. (3) for DBP would require a nine-dimensional integral to remove x_2 – x_{10} from the posterior. Markov Chain Monte Carlo methods, such as the Metropolis algorithm (Robert and Casella, 2013), generate a representative sample of the posterior without direct calculation or integration. The means of the resultant sample are then used to determine new values of θ.

4.1. Metropolis algorithm

The Metropolis algorithm samples the posterior PDF by performing a random walk through the parameter space and assessing the performance of each randomly generated parameter vector. New, candidate vectors θ_{can}, are generated from a Multivariate Gaussian proposal distribution with mean vector equal to the previous parameter vector, θ_0, and some predefined variance-covariance matrix, V (Chib and Greenberg, 1995). The parameter space explored by the algorithm is defined by the prior distributions assigned to the parameters and the average step size,

Table 11
Performance of calibrated traction equation.

Performance	Calibration set R^2	Calibration set RMSE	Test set R^2	Test set RMSE
VTI model	0.826	0.060	0.743	0.068
Calibrated model	0.831	0.057	0.741	0.066
% Improvement	0.6%	5.5%	−0.3%	2.5%

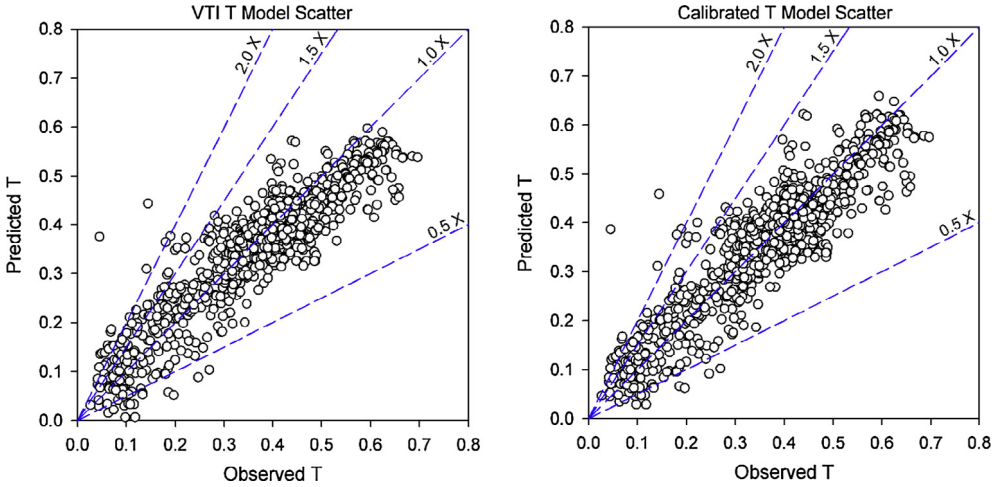

Fig. 8. VTI and calibrated model scatter plots for traction.

Table 12
Gaussian prior distributions for exploration of motion resistance equation.

MR	x_1	x_2	x_3	x_4	x_5	x_6
μ	0.5	0.002	0.5	0.002	5e−5	0.008
σ_i^2	0.15	0.0006	0.15	0.0006	1.5e−5	0.0024

Table 13
Initial and final exploration chain means for motion resistance.

Gaussian	x_1	x_2	x_3	x_4	x_5	x_6
Initial	0.5	0.002	0.5	0.002	5e−5	0.008
Chain 1	0.33	0.0014	0.26	0.0014	2.37e−5	0.0125
Chain 2	0.35	0.0018	0.30	0.0018	8.25e−5	0.0095
Chain 3	0.36	0.0017	0.28	0.0016	3.37e−5	0.0090
Chain 4	0.36	0.0017	0.27	0.0016	4.30e−5	0.0091
Chain 5	0.34	0.0014	0.27	0.0013	5.55e−5	−0.0009

dictated by V. The unbounded proposal distribution may occasionally generate a candidate vector outside the parameter space when prior PDFs are defined using bounded distributions. If there are no correlations between parameters in the proposal distribution, that is V is diagonal and the distribution symmetric, the infeasible candidate vector may be reflected back into the feasible parameter space (Van Oijen, 2008).

Whether or not a candidate vector is stored by the algorithm is determined based on its performance through the Metropolis ratio, $\gamma = P_{can}L_{can}/(P_0L_0)$, where P_{can} and L_{can} are the prior PDF and likelihood functions of the candidate points, respectively, and P_0 and L_0 the same for the previous vector. A candidate vector with $\gamma > 1$ is always accepted, while those with $\gamma < 1$ are randomly accepted with probability equal to their metropolis ratio, γ. The ability to randomly accept candidate points that do not demonstrate improvement prevents the random walk from becoming stuck on a single candidate point. The process of generating candidate vectors and accepting or rejecting them is repeated n times, the length of the Markov chain, and the final set of accepted parameter vectors is referred to as the chain, denoted by θ^n.

Once the posterior PDF has been sufficiently sampled by the Metropolis algorithm, the initial search phase of the chain, generally the first 10%, must be removed to ensure accurate calculation of the parameter means (Van Oijen, 2008). Convergence is established through visual inspection of the trace plots of the parameters and comparison of the

Table 14
Original VTI values and prior distribution bounds for coefficients in motion resistance equation.

MR	x_1	x_2	x_3	x_4	x_5	x_6
VTI	0.44	2.287e−3	0.44	2.287e−3	4.57e−5	0.008
LB	0.20	0.0008	0.15	0.0008	−0.00001	−0.05
UB	0.40	0.0020	0.45	0.0020	0.00010	0.10

intra- and inter-chain variances for multiple chains. Trace plots are inspected to verify that acceptance of candidate coefficient vectors is dominated by the random acceptance of the Metropolis algorithm rather than improved performance of candidate vectors. An example of a non-converged trace plot is given in Fig. 2, while a converged trace plot is illustrated in Fig. 3 where new steps in the Markov Chain appear along the horizontal axes and the value taken by a given calibration parameter captured on the vertical axes. The inter- and intra-chain variances are evaluated to show that the variance of accepted candidate vectors between multiple chains is less than the variance within a single chain, indicating those chains have converged to a single solution. That is, when the variance within a single chain, the inter-chain variance, is less than the variance between multiple chains, the intra-chain variance, then it is concluded the chains have converged.

A general form of the Metropolis algorithm is given in Fig. 4 (Van Oijen, 2008; Van Oijen et al., 2005), and the BC process for calibrating equations from the VTI model is illustrated in Fig. 5. For a more detailed discussion of the Metropolis algorithm, see Robert and Casella (2013).

4.2. Two-stage calibration method

The parameter space explored by the Metropolis algorithm is defined by the prior PDFs of θ. Uniform prior PDFs represent a minimum assumption of information and were desired for θ; however, lack of physical meaning and bounds for the parameters in the empirical models suggested non-bounded prior PDFs, like the Gaussian distribution, might be more appropriate. The Gaussian distributions required assumptions about the most-likely best values of θ, but explored model performance in an unrestricted parameter space. Uniform distributions, in addition to representing a minimum assumption of information, more thoroughly explored a limited parameter space than the Gaussian distributions. A two-stage calibration method was implemented to combine the advantages of both choices for prior PDFs.

Gaussian prior PDFs with large standard deviations were used to explore the parameter space and determine initial bounds for parameters in a first-stage calibration. A strict rule for defining the means of the Gaussian distributions was not established, as the standard deviations, chosen to allow significant departure from the original values, were more critical to the Markov Chains than their starting points. The parameters in θ were considered independent, reducing V to a diagonal matrix defined as

$$V_{ii} = a\sigma_i^2 \tag{11}$$

where σ_i is the standard deviation of the ith parameter in θ and a is used to adjust the step size. Five chains were run from the initial values of θ to more rapidly explore the parameter space. Convergence and validation were not considered priorities during the first stage, and therefore the full subsets of data available from DROVE were used for each equation. The decision process of calibrating, adjusting variables, and recalibrating in the first stage is shown in Fig. 6.

Uniform PDFs initially defined using the boundaries from the first stage were used in a second stage calibration to give the final, calibrated form of the equations. The bounds of the Uniform PDFs were adjusted throughout the second calibration stage to produce the best, converged, values of θ. Similar to the first stage, V was defined in Eq. (12) as a diagonal matrix using the upper and lower bounds (UB and LB) of the prior PDFs and an adjustable coefficient, c.

$$V_{ii} = c(UB - LB)^2 \tag{12}$$

The second calibration stage was completed using three chains with starting points that evenly divided the bounds of the prior PDFs. The coefficients of θ were considered final and the calibrated equations defined once both convergence criteria were satisfied and the improved performance of the new equation was validated using the test datasets.

Table 15
Original VTI and mean values for coefficients in motion resistance equation with uniform priors.

Uniform	x_1	x_2	x_3	x_4	x_5	x_6
Chain 1	0.30	0.0016	0.27	0.0016	4.47e−5	0.028
Chain 2	0.30	0.0018	0.27	0.0018	4.42e−5	0.040
Chain 3	0.29	0.0017	0.27	0.0017	5.29e−5	0.037
Average	0.30	0.0017	0.27	0.0017	4.72e−5	0.035

5. Calibration results

5.1. Drawbar pull

To reduce the number of independent coefficients considered in calibration, repeated values in Eq. (1) for DBP remained linked in the coefficient form of the equation, Eq. (3). The distribution parameters of the Gaussian priors for the ten coefficients in Eq. (3) used in the first calibration stage are provided in Table 2.

The V of the proposal distribution was defined according to Eq. (11) with $a = 0.1$ after several trials. First-stage calibration with $n = 10{,}000$ resulted in the coefficient means presented in Table 3, which also captures the anticipated problem of calibrating those parameters in Eq. (3) that disappear when $\alpha = 0$: x_3, x_4, x_5, x_7, x_8, and x_{10}.

The bounds initially defined with the aid of Table 3 were adjusted through several trials in the second stage to achieve convergence. The final lower and upper bounds of the Uniform prior PDFs as well as the original VTI coefficients for Eq. (3) are provided in Table 4.

The second calibration stage was completed using $n = 100{,}000$ and V of the proposal distribution defined with $c = 0.1$ in Eq. (12). Trace plots for each coefficient in the three chains were visually inspected and found to

Table 16
Performance of calibrated motion resistance equation.

Performance	Calibration set R^2	Calibration set RMSE	Test set R^2	Test set RMSE
VTI model	0.62	0.105	0.62	0.111
Calibrated model	0.64	0.081	0.63	0.085
% Improvement	2.5	23.1	2.2	23.9

show convergence, while the inter-chain variance was found to be less than the intra-chain variance for all three chains. The means of the second-stage chains are presented in Table 5.

The average of the three chains, as shown in the last row of Table 5, gives the final, calibrated equation, which was compared to the root-mean square error (RMSE) and the coefficient of determination (R^2) performance of the equation provided in the VTI model in Table 6.

The calibrated equation represents an improvement over the original VTI equation, shown by a 17.3% improvement in RMSE and 2.82% improvement in R^2 performance, both validated through the test set as illustrated in Table 6. Scatter plots demonstrating contraction toward a 1:1 relationship of the observed and predicted values when moving from the VTI to calibrated equation are presented in Fig. 7.

The final calibrated equation for DBP of off-road vehicles in loose sands is given as

$$\mathrm{DBP} = 0.53 + \frac{0.011}{s} - 5.41\alpha^{0.92-8.35s} - \frac{\left(0.53 + \frac{0.011}{s} - 5.41\alpha^{0.92-8.35s}\right)(12.55 - 10\alpha^2)}{N_s - \frac{1.33}{s^{\frac{1}{3}}} + \frac{5.28}{s}\alpha^3 + 12.55 - 10\alpha^2} \quad (13)$$

5.2. Traction

The T equation from the VTI model was seen to perform significantly better with regard to RMSE and R^2 than the DBP and MR equations, presenting challenges in calibrating the equation. First, standard deviations for the Gaussian prior PDFs had to be large enough to allow exploration of new parameter spaces, while not being so large as to prohibit sufficient exploration near the original parameter values. These competing requirements were somewhat mitigated by extending the length of the first-stage chains from $n = 10{,}000$ to $n = 20{,}000$. The parameters of the Gaussian priors used in the first-stage calibration of the T equation are presented in Table 7.

Similar difficulties were encountered in defining V for the proposal distribution, and eventually $a = 0.0125$ in Eq. (11) was used to define V after several iterations. The initial and final means for the five first-stage chains are shown in Table 8.

Almost universal movement away from the VTI values of x_1 resulted in initial bounds which excluded the initial VTI coefficients. Refinement of the bounds of the Uniform prior PDFs resulted in a similar exclusion of the VTI value by the bounds of x_2. The bounds of the second-stage Uniform prior PDFs, after first-stage-guided adjustments to facilitate convergence, are reported in Table 9 alongside the initial VTI coefficients.

The final matrix V for the three second-stage chains, $n = 100{,}000$, was defined according to Eq. (12) with $c = 0.04$. The resultant chain means for the second calibration stage are presented in Table 10. Trace plots for each parameter were examined and found to show convergence, while the inter-chain variance was found to be less than the intra-chain variance for all three chains.

The performance of the calibrated equation, with coefficients taken to be the average of the three chains, and the equation in the VTI model are compared in Table 11.

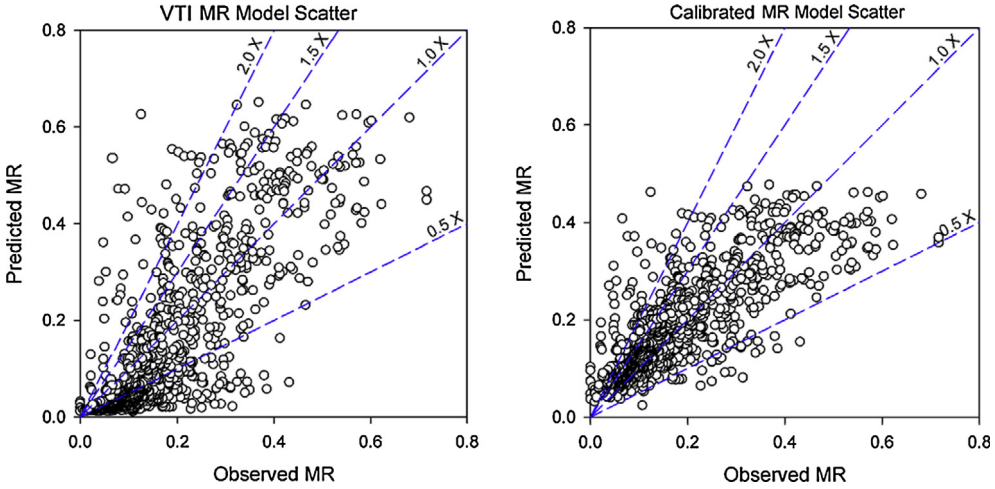

Fig. 9. VTI and calibrated model scatter plots for motion resistance.

The original T equation from the VTI model captures a large amount of the variation in the available data for loose, dry sands and leaves little room for improvement through coefficient adjustment alone. Some reduction in RMSE was achieved, 5.5%, with both equations performing similar with regard to R^2. Scatter plots of the observed and predicted values for both models are presented in Fig. 8 and demonstrate the similarity in performance between the two models.

The final calibrated T model is presented as

$$T = 0.77 - \frac{1.09\left(3.8 + \frac{2.17}{s}\right)}{N_s + 10.5 + \left(7.93 + \frac{3.14}{s}\right)} \tag{14}$$

5.3. Unpowered motion resistance

Unlike the T equation, the poor performance of the VTI model for MR with regard to RMSE and R^2 allowed for significant improvement through coefficient adjustment. The parameters of the Gaussian prior PDFs for first-stage calibration are presented in Table 12.

The standard deviations for the Gaussian prior PDFs of each parameter were defined to allow for a broad investigation of the parameter space while generating new parameter values of similar magnitude to the initial point. The proposal distribution was defined for the $n = 10{,}000$ chains in the first stage with $a = 0.1$ in Eq. (11). Initial and final mean values for the five exploration chains are presented in Table 13.

Significant adjustments to the boundaries of the Uniform prior PDFs were required to achieve convergence. The final boundaries for the Uniform prior PDFs used in the second stage are reported in Table 14 along with the original VTI values.

The matrix V for the proposal distribution was defined according to Eq. (12) with $c = 0.02$ for the three $n = 100{,}000$ second-stage chains after several iterations. The final calibrated coefficient values for each of the three chains are presented in Table 15.

Trace plots for each coefficient were examined and found to have converged. Additionally, the inter-chain variance was seen to be less than the intra-chain variance for all three chains. The performance of the calibrated equation and the equation for MR from the VTI model are compared in Table 16.

The low amount of variability captured by the MR equation in the VTI model suggests a problem with the equation structure or implementation rather than the equation coefficients. Even so, the Metropolis algorithm was able to give a coefficient vector for Eq. (8) which improved the equation's RMSE performance by 23% and R^2 performance by 2.5%, with both improvements validated by the test set. Scatter plots of the observed vs. predicted values for both equations are presented in Fig. 9.

The final calibrated model for motion resistance is given as

$$MR = 0.30 - 0.0017N_{s,u} + \sqrt{(0.27 - 0.0017N_{s,u})^2 + 0.0000472N_{s,u} + 0.035} \tag{15}$$

6. Conclusions

In this study, Bayesian Calibration, along with a recently developed database, DROVE, was used to improve the VTI model equations for estimating the coefficients of drawbar pull, traction, and motion resistance. The large amount of data on vehicle performance over loose, dry sand available for calibration allowed for improvement in all three of the equations considered from the VTI model.

The calibrated equation for DBP showed a 17.3% improvement in RMSE and a 2.8% improvement in R^2. Calibration of the T equation resulted in a 5.5% improvement to RMSE with similar R^2 performance to the original equation. For the MR equation, improvements of 23.1% in RMSE and 2.5% in R^2 were demonstrated for the calibrated equation.

Limitations do, however, exist for each of the three equations. For DBP the small amount of steering data available, just 37 of more than 1000 total observations, suggests a more thorough investigation for steered vehicles is required in order to ensure the effect of steering is adequately captured by the calibrated equation. The performance of the VTI equation for T on the DROVE dataset left little room for improvement through coefficient calibration alone, although some validated improvement was shown in RMSE performance. It was not possible to validate improvements in R^2 performance of the calibrated T equation over the VTI equation, although the performance was shown to be at least similar. For MR, the scatter plot of observed versus predicted values for the equation from the VTI model indicates a flaw in the basic structure of the model, as does its RMSE and R^2 when applied to the dataset. As previously stated, the Bayesian calibration process only provides improved coefficients for a given equation; it cannot change the structure of the equation itself.

Despite these limitations, improvements to the three equations (DBP, T, and MR) were validated through a combination of factors. First, trace plots of the coefficient chains were visually inspected to verify that acceptance of candidate coefficient vectors was dominated by the random nature of the Metropolis algorithm rather than the performance of the vectors. Second, multiple chains were run for the coefficients and converged to a single solution, verified through comparison of the inter- and intra-chain variances. Third, the calibrated equations were validated against the originals from the VTI model using a test dataset set aside from the data used to calibrate the models. The T equation was the only calibrated equation which did not show validated improvement in the coefficient of determination, although performance was established to be, at a mini-

mum, similar. Taken together, these factors provide enough evidence to accept the proposed calibrated equations for the coefficients of drawbar pull, traction, and motion resistance as improvements to those provided in the VTI model for vehicles operating in loose sands.

Acknowledgments

This effort was sponsored by the Engineering Research & Development Center under Cooperative Agreement number W912HZ-15-2-0004. The views and conclusions contained herein are those of the authors and should not be interpreted as necessarily representing the official policies or endorsements, either expressed or implied, of the Engineering Research & Development Center or the U.S. Government. This paper is based on the work conducted under Task 12: Mobility Modeling for Soils. Roger King, Director of the Center for Advanced Vehicular Systems (CAVS) at Mississippi State University, was principal investigator for W912HZ-15-2-0004 and Farshid Vahedifard was the lead for Task 12.

References

Ahlvin, R.B., Haley, P.W., 1992. NATO Reference Mobility Model Edition II, NRMM II User's Guide (Technical Report No. GL-92-19). U.S. Army Engineer Waterways Experiment Station, Vicksburg, MS.

Chib, S., Greenberg, E., 1995. Understanding the Metropolis Hastings Algorithm. Am. Stat. 49, 327–335. http://dx.doi.org/10.2307/2684568.

Durham, G.N., 1976. Powered Wheels in the Turned Mode Operating on Yielding Soils (Technical Report No. M-76-9). U.S. Army Engineer Waterways Experiment Station, Vicksburg, MS.

Freitag, D.R., Knight, S.J., 1964. A Technique for Estimating the Slope-Climbing Ability of Wheeled Vehicles in Sand (Technical Report). SAE Technical Paper.

Geotechnical Laboratory, 1960. The Unified Soil Classification System (Technical Memorandum No. 3–357). U.S. Army Engineer Waterways Experiment Station, Vicksburg, MS.

Jones, R.A., McKinley, G.B., Richmond, P.W., Creighton, D.C., Ahlvin, R.B., Nunez, P., 2007. A vehicle terrain interface. In: Proceedings of the Joint North America, Asia-Pacific ISTVS Conference and Annual Meeting of Japanese Society for Terramechanics. Presented at the Joint North America, Asia-Pacific ISTVS Conference and Annual Meeting of Japanese Society for Terramechanics, Fairbanks, AK.

Kass, R.E., Wasserman, L., 1996. The selection of prior distributions by formal rules. J. Am. Stat. Assoc. 91, 1343–1370. http://dx.doi.org/10.1080/01621459.1996.10477003.

Kennedy, M.C., O'Hagan, A., 2001. Bayesian calibration of computer models. J. R. Stat. Soc. 63, 425–464. http://dx.doi.org/10.1111/1467-9868.00294.

Lee, P.M., 2012. Bayesian Statistics, An Introduction. John Wiley & Sons.

Lee, J.H., 2015. Statistical modeling and comparison with experimental data of tire–soil interaction for combined longitudinal and lateral slip. J. Terramech. 58, 11–25. http://dx.doi.org/10.1016/j.jterra.2014.12.005.

MacLeod, P., 2001. The Availability and Capabilities of "Low-End" Virtual Modelling (Prototyping) Products to Enable Designers and Engineers to Prove Concept Early in the Design Cycle. Prime Faraday Partnership.

Melzer, K.-J., 1971. Measuring Soil Properties in Vehicle Mobility Research. Report 4. Relative Density and Cone Penetration Resistance. DTIC Document.

Melzer, K.-J., 1976. Performance of Towed Wheels Operating in Turned Mode on Soft Soils–A Pilot Study. (Miscellaneous Paper No. M-76-17). U.S. Army Engineer Waterways Experiment Station, Vicksburg, MS.

Meyer, M.P., Ehrlich, I.R., Sloss, D., Murphy Jr., N.R., Wismer, R.D., Czako, T., 1977. International Society for terrain-vehicle systems standards. J. Terramech. 14, 153–182.

O'Hagan, A., 2006. Bayesian analysis of computer code outputs: a tutorial. Reliab. Eng. Syst. Saf. 91, 1290–1300. http://dx.doi.org/10.1016/j.ress.2005.11.025.

Priddy, J.D., 1999. Improving the Traction Prediction Capabilities in the NATO Reference Mobility Model (NRMM). (Technical Report No. GL-99-8). U.S. Army Engineer Waterways Experiment Station, Vicksburg, MS.

Robert, C., Casella, G., 2013. Monte Carlo Statistical Methods. Springer Science & Business Media.

Rohde, M.M., Crawford, J., Toschlog, M., Iagnemma, K.D., Kewlani, G., Cummins, C.L., Jones, R.A., Horner, D.A., 2009. An interactive physics-based unmanned ground vehicle simulator leveraging open source gaming technology: progress in the development and application of the virtual autonomous navigation environment (VANE) desktop. In: Gerhart, G.R., Gage, D.W., Shoemaker, C.M. (Eds.), Presented at the Unmanned Systems Technology XI, Orlando, FL, p. 73321C. http://dx.doi.org/10.1117/12.820069.

Schreiber, M., Kutzbach, H.D., 2008. Influence of soil and tire parameters on traction. Res. Agr. Eng. 54, 43–49.

Schreiner, B.G., Moore, D.W., Grimes, K., 1985. Mobility Assessment of the Heavy Expanded Mobility Tactical Truck (HEMTT)-Initial Production Vehicle (Technical Report No. GL-85-4). U. S. Army Engineer Waterways Experiment Station, Vicksburg, MS.

Stone, M., 1974. Cross-validatory choice and assessment of statistical predictions. J. R. Stat. Soc. Methodol. 36, 111–147.

Taheri, S., Sandu, C., Taheri, S., Pinto, E., Gorsich, D., 2015. A technical survey on Terramechanics models for tire–terrain interaction used in modeling and simulation of wheeled vehicles. J. Terramech. 57, 1–22. http://dx.doi.org/10.1016/j.jterra.2014.08.003.

Turnage, G.W., 1972. Performance of Soils under Tire Loads. Report 8. Application of Test Results to Tire Selection for Off-Road Vehicles (Technical Report No. 3–666). U. S. Army Engineer Waterways Experiment Station, Vicksburg, MS.

Turnage, G.W., 1995. Mobility Numeric System for Predicting In-the-Field Vehicle Performance (Miscellaneous Paper No. GL-95-12). U.S. Army Engineer Waterways Experiment Station, Vicksburg, MS.

Vahedifard, F., Robinson, J.D., Mason, G.L., Howard, I.L., Priddy, J.D., 2016. Mobility algorithm evaluation using a consolidated database developed for wheeled vehicles operating on dry sands. J. Terramech. 63, 13–22. http://dx.doi.org/10.1016/j.jterra.2015.10.002.

Vahedifard, F., Mason, G.L., Howard, I.L., Priddy, J.D., 2017. Development of a multi-year database to assess off-road mobility algorithms in fine-grained soils. Int. J. Veh. Perform. 3, 3–18.

Van Oijen, M., Rougier, J., Smith, R., 2005. Bayesian calibration of process-based forest models: bridging the gap between models and data. Tree Physiol. 25, 915–927.

Van Oijen, M., 2008. Bayesian Calibration (BC) and Bayesian Model Comparison (BMC) of Process-Based Models: Theory, Implementation and Guidelines.

Vong, T.T., Haas, G.A., Henry, C.L., 1999. NATO Reference Mobility Model (NRMM) Modeling of the DEMO II Experimental Unmanned Ground Vehicle (XUV) (Technical Report No. ARL-MR-435). U.S. Army Research Laboratory, Aberdeen Proving Ground, MD.